

Radio limits on off-axis GRB afterglows and VLBI observations of SN 2003gk

M. F. Bietenholz,^{1,2★} F. De Colle,³ J. Granot,⁴ N. Bartel² and A. M. Soderberg⁵

¹Hartebeesthoek Radio Observatory, PO Box 443, Krugersdorp 1740, South Africa

²Department of Physics and Astronomy, York University, Toronto, ON M3J 1P3, Canada

³Instituto de Ciencias Nucleares, Universidad Nacional Autónoma de México, A. P. 70-543 04510 D. F., Mexico

⁴Department of Natural Sciences, The Open University of Israel, 1 University Road, PO Box 808, Ra'anana 43537, Israel

⁵Harvard-Smithsonian Center for Astrophysics, 60 Garden Street, Cambridge, MA 02138, USA

Accepted 2014 February 4. Received 2014 January 16; in original form 2013 October 24

ABSTRACT

We report on a Very Large Array survey for late-time radio emission from 59 supernovae (SNe) of the Type I b/c, which is associated with long-duration gamma-ray bursts (GRBs). An ‘off-axis’ GRB burst (i.e. whose relativistic jet points away from us) is expected to have late-time radio emission even in the absence of significant prompt gamma-ray emission. From our sample, we detected only SN 2003gk with an 8.4 GHz flux density of $2260 \pm 130 \mu\text{Jy}$. Our subsequent very long baseline interferometry (VLBI) observations of SN 2003gk, at an age of ~ 8 yr, allowed us to determine its radius to be $(2.4 \pm 0.4) \times 10^{17}$ cm, or 94 ± 15 light days. This radius rules out relativistic expansion as expected for an off-axis GRB jet, and instead suggests an expansion speed of $\sim 10\,000 \text{ km s}^{-1}$ typical for non-relativistic core-collapse SNe. We attribute the late-onset radio emission to interaction of the ejecta with a dense shell caused by episodic mass-loss from the progenitor.

In addition, we present new calculations for the expected radio light curves from GRB jets at various angles to the line of sight, and compare these to our observed limits on the flux densities of the remainder of our SN sample. From this comparison, we can say that only a fraction of broadlined Type I b/c SNe have a radio-bright jet similar to those seen for GRB afterglows at cosmological distances. However, we also find that for a reasonable range of parameters, as might be representative of the actual population of GRB events rather than the detected bright ones, the radio emission from the GRB jets can be quite faint, and that at present, radio observations do not place strong constraints on off-axis GRB jets.

Key words: supernovae: individual: (SN 2003gk) – radio continuum: general.

1 INTRODUCTION

Long-duration gamma-ray bursts (GRBs) are thought to involve the highly directed relativistic ejection of material from a collapsing massive star, in other words the formation of relativistic jets. The observed gamma-ray emission is produced within the outflow, outside of the progenitor star but before there is significant deceleration by the surrounding medium. The ejected material interacts with the circumstellar material (CSM) and strong shocks are produced. These shocks amplify the magnetic field and accelerate particles to relativistic energies, the combination of which results in synchrotron emission. For reviews of GRBs, see for example Piran

(2004), Mészáros (2006), Granot (2007) and Gehrels, Ramirez-Ruiz & Fox (2009).

A GRB is observed when such a jet is directed close to the line of sight, and strong Doppler boosting is responsible for the characteristic bright gamma-ray emission. It follows from this model, however, that the majority of GRB events have jets which are not oriented near the line of sight, and therefore go undetected (Rhoads 1997; Granot et al. 2002; Nakar, Piran & Granot 2002), with Frail et al. (2001) estimating that >99 per cent of GRB events go undetected.

However, on the basis of several nearby ($z < 0.3$) long-duration GRBs it has been established that they are associated with supernovae (SNe) of Type Ib/c, which are ones from a progenitor star that has lost much of its envelope prior to the explosion (e.g. Galama et al. 1998; Stanek et al. 2003; Malesani et al. 2004; Pian et al. 2006; Cobb et al. 2010; Starling et al. 2011; Xu et al. 2013). In addition, there is indirect evidence for this association, such as large ongoing

★E-mail: mbieten@yorku.ca

specific star formation rates at the location of the GRBs in their host galaxies, or late-time red bumps in their afterglow light curves (see, e.g. Woosley & Bloom 2006, and references therein). These events therefore feature both highly collimated relativistic jets giving rise to the GRB and an associated more isotropic and non-relativistic SN explosion. This duality underlies the popular ‘collapsar’ model (Woosley 1993; MacFadyen, Woosley & Heger 2001) in which a central engine (accreting, rapidly spinning compact object) drives the relativistic jets while the spherical SN explosion is powered by neutrinos.

GRB events, in addition to the gamma-ray emission, also produce longer-lived emission at lower frequencies, called the afterglow. In particular, afterglows are often detected in radio (see, e.g. van Paradijs, Kouveliotou & Wijers 2000; Zhang 2007). As the GRB decelerates to mildly or sub-relativistic speeds, it produces strong, nearly isotropized, radio emission. The radio emission is much less strongly beamed than the gamma-ray emission, and so in the radio ‘off-axis’ events are not significantly more difficult to detect than on-axis ones at sufficiently late times. Indeed, it has been shown that the radio is probably the best wavelength range for detecting such off-axis events (e.g. Paczyński 2001; Granot & Loeb 2003).

Models of off-axis GRB events developed so far have typically showed that, for angles to the line of sight of 30° to 90° , the radio brightness peaks ~ 1 to ~ 2 yr after the explosion (Granot & Loeb 2003; van Eerten, Zhang & MacFadyen 2010). Future large-area surveys with instruments such as ASKAP, LOFAR, MeerKAT, and of course SKA, will likely detect such off-axis events in blind surveys. At present, however, detection in a blind survey is challenging, and radio observations are mostly restricted to follow-up observations of events previously detected in other wavelengths (see Chandra & Frail 2012, and references therein).

Type I b/c SNe provide the ideal locations to search for off-axis GRB events. Since non-relativistic SNe can also produce radio emission, some means of distinguishing the radio emission from putative off-axis jet from that of the normal SN is needed. In the models available at present, the time-scales of the two processes are notably different and could therefore provide the necessary discriminant. In particular, the models suggested that radio emission from an off-axis event had a relatively long interval between the explosion and the time of maximum radio emission, so that for angles to the line of sight of 30° to 90° , the peak radio brightness typically occurs ~ 1 to ~ 2 yr after the explosion (van Eerten et al. 2010; Granot & Loeb 2003). The radio emission from normal Type I b/c SNe, on the other hand, has short time-scales, with rise-times at 8.4 GHz of typically a few weeks to months after the explosion, followed by a relatively rapid decay with flux density, S approximately $\propto t^{-1.5}$ (Weiler et al. 2002; Chevalier & Fransson 2006). Off-axis GRB events are also distinguished by having high peak spectral luminosities, generally $> 10^{28}$ erg s $^{-1}$ Hz $^{-1}$ (8.4 GHz), while those of normal Type I b/c SNe are mostly $< 10^{28}$ erg s $^{-1}$ Hz $^{-1}$, although some very radio bright normal SNe are known (see, e.g. Soderberg 2007), such as SN 2003L (Soderberg et al. 2005).

The models therefore suggested that late-onset and luminous radio emission from a Type I b/c SN could be used as a signpost of an off-axis GRB event. Soderberg et al. (2006a) carried out a search for such events, and observed 68 Type I b/c SNe in the radio at late times. They did not detect any radio emission and concluded that only a fraction of < 10 per cent of all Type I b/c SN are associated with a bright GRB jet regardless of orientation. They could also rule out, at the 84 per cent confidence level, the hypothesis that all of the subset of Type I b/c SNe which had broad absorption lines and are therefore classified as ‘broadlined’ (sometimes also termed

‘hypernovae’) such as SN 2003jd or SN 2002ap, are associated with GRB events.

Should late-onset radio emission be detected from a Type I b/c, and important diagnostic would be the size of the radio emitting region. If it is indeed due to a relativistic jet, sizes of the order of one light-year are expected. Non-relativistic SNe, however, expand much more slowly, typically with initial speeds of $0.1c$ and average speeds of the order of $10\,000$ km s $^{-1}$ over periods of > 1 yr, and would therefore about an order of magnitude smaller.

Indeed there have been several Type I b/c SNe suspected of possibly harbouring an off-axis GRB where subsequent very long baseline interferometry (VLBI) observations showed that there was *no* relativistic expansion (see Bietenholz 2014, for a recent review of VLBI observations of Type I b/c SNe). SN 2001em showed late-onset radio emission but the VLBI observations implied only non-relativistic expansion (Granot & Ramirez-Ruiz 2004; Bietenholz & Bartel 2005, 2007; Schinzel et al. 2009). The late turn-on radio emission from SN 2001em was subsequently interpreted as radio emission produced by the interaction of normal (non-relativistic) Type I b/c ejecta with a massive and dense circumstellar shell located at some distance from the progenitor, produced by mass-loss from the latter, perhaps due to an eruptive event like those of luminous blue variables (Chugai & Chevalier 2006; Chevalier 2007). SN 2007bg and the supernova PTF 11gcj also showed late-onset radio-emission (Salas et al. 2013; Corsi et al. 2014) that is also attributed to the interaction of a non-relativistically expanding shock with dense shells of CSM produced by episodic mass-loss of the progenitor. In another case, SN 2007gr, it was initially claimed that the VLBI observations implied relativistic expansion (Paragi et al. 2010); however, Soderberg et al. (2010b) subsequently suggested that all the observations could be explained by an ordinary, non-relativistically expanding SN.

In a third nearby Type I b/c SN, SN 2009bb, the high radio luminosity also suggested relativistic ejection (Soderberg et al. 2010a). In this case, the VLBI observations were consistent with, but did not demand, mildly relativistic expansion (Bietenholz et al. 2010b).

The radio light curve of a non-relativistic SN generally has a steep rise, as the radio emission is initially absorbed by either synchrotron self-absorption or, less commonly for Type I b/c SNe, by free-free absorption due to an optically thick CSM (see, e.g. Chevalier 1998). Once the SN has become optically thin at the frequency of interest, the light curve generally decays. The canonical model of Chevalier (1982), which assumes power-law radial density profiles for both the CSM and the ejecta, produces a power-law decay in the light curve after the peak. The interval between the explosion and the peak radio brightness is a function of the observing frequency, generally being longer at lower frequencies. It should however, be noted, that significant departures from a strictly power-law decline in the radio emission are relatively common (e.g. SN 2009bb Bietenholz et al. 2010b, SN 1996cr Meunier et al. 2013, SN 1986J, Bietenholz, Bartel & Rupen 2002, 2010, SN 1979C Bartel & Bietenholz 2008).

As there are as yet no confirmed examples of off-axis GRB jets without a detected gamma-ray signature, it would be very important to detect one, or, even in the absence of a detection to set limits on the fraction of Type I b/c SNe which are associated with a relativistic ejection. Earlier work by Soderberg et al. (2006a), Soderberg, Frail & Wieringa (2004) and Gal-Yam et al. (2006) showed that at most a small fraction of Type I b/c can be associated with bright jets typical of detected cosmological GRBs. Nonetheless, if the current paradigm of GRBs involving highly directed ejection is correct, then for every observed GRB there must be many as yet unobserved off-axis events. Searching for late-time radio emission seems a

relatively promising way to detect such an event, despite the knowledge that many Type I b/c SNe will have to be searched to obtain one detection.

We therefore undertook a radio survey of Type I b/c SNe with ages between 1 and 8 yr to look for late-time radio emission using the National Radio Astronomy Observatory (NRAO) Very Large Array (VLA). In Section 2, we describe this survey and give the results. One object, SN 2003gk, was detected, and in Section 3 we discuss our followup VLA and VLBI observations of SN 2003gk. In Section 4, we calculate new model radio light curves for off-axis GRB jets, and compare them to our observations in Section 5. We discuss the implications of our results in Section 6, and summarize our conclusions in Section 7.

2 SURVEY FOR LATE-TIME RADIO EMISSION FROM TYPE I B/C SUPERNOVAE

2.1 VLA survey observations

We used the VLA to survey a sample of 59 Type I b/c SNe with declinations $> -30^\circ$ and with ages between 1 and 8 yr, for late-time radio emission. We chose ordinary Type I b/c SNe only at distances < 80 Mpc, but we also observed several Type I b/c SNe of the ‘broadlined’ subtype which is most reliably associated with GRBs out to slightly larger distances up to 120 Mpc. Our sample is not intended to be complete, merely representative.

We observed in two sessions of 4 h each, on 2009 May 28 and May 29 (observing code AB1327). The array was in the CnB transitional configuration, and we observed with a total bandwidth of 100 MHz around a central frequency of 8.435 GHz. The data reduction was carried out in the standard way, using 3C 48 and 3C 286 as flux-density calibrators on the two days, respectively (using the VLA 1999.2 flux-density scale). Each SN was observed for ~ 7.3 min, with phase calibration derived from bracketing scans of a nearby compact calibrator sources.

After calibration, we imaged the SNe. If there was sufficient flux density in the field, self-calibration in phase was attempted. However, the improvements in the SN images achieved by self-calibration ranged from non-existent to insignificant, suggesting that our initial phase-calibration is generally adequate for our purposes. Both the effective resolution and image background rms values varied from one SN to the other. The full width at half-maximum (FWHM) areas of the convolving beam ranged from ~ 3.5 to ~ 12 arcsec², and image rms values from ~ 50 to ~ 100 μJy bm^{-1} . We can consider the SN positions accurately known for our purposes, since the coordinates of the SNe were obtained from optical observations, and are usually accurate to an arcsecond or better, and the position errors due to the VLA phase referencing are also expected to be < 1 arcsec, whereas the FWHM resolution of the radio observations was mostly > 2 arcsec.

2.2 VLA survey results

We present our flux-density measurements, or upper limits, for each of the SNe in Table 1. As an uncertainty in the flux density we take the background rms or the radio image. With the exception of SN 2003gk, which is discussed below, we detected none of our sample SNe. Since, as mentioned, the SN positions are accurately known, we take the brightness of the radio image at the SN position as an estimate of the SN’s flux density. If this flux density is less than the flux-density uncertainty, we give only 3σ upper limit on the flux density in Table 1. In the cases where the flux density exceeds

the image rms, we give the estimate of the flux density as well as its uncertainty in addition to the 3σ limit.

The only reliably detected source was SN 2003gk. The observed morphology is consistent with being unresolved (as expected), with a flux density of 2260 ± 130 μJy bm^{-1} , where the uncertainty consists of the image rms and a 5 per cent calibration uncertainty added in quadrature.

For the other 58 SNe, the 3σ upper limits given in Table 1 are conservative upper limit on the flux density of the SN since the presence of extended emission due to the galaxy cannot be ruled out. We note that in several cases, galactic emission is clearly seen at the SN location, and our limit on the SN emission is the limit on any compact emission in excess of the galactic emission at the SN location. No unresolved sources (except for SN 2003gk) were seen within several arcseconds of the nominal locations of any of our SNe.

From our measurements and limits to the flux density, we calculate the corresponding values of or limits on the radio spectral luminosity at 8.5 GHz using the distances indicated in Table 1. We plot these values in Fig. 1. The luminosity of SN 2003gk was $(5.6 \pm 0.3) \times 10^{27}$ erg s^{-1} Hz^{-1} (where the uncertainty does not include any uncertainty in the distance, which was taken to be 44 Mpc).

We note that our survey is similar to that of Soderberg et al. (2006a), who also obtained upper limits on the 8.5 GHz flux density and thus radio luminosity of Type I b/c SNe at late times. We in fact re-observed 14 SNe from that earlier survey: SN 2001ej, SN 2001is, SN 2002J, SN 2002bl, SN 2002cp, SN 2002hf, SN 2002ho, SN 2002hy, SN 2002hz, SN 2002ji, SN 2002jj, SN 2002jp, SN 2003dr and SN 2003jd. Our flux-density limits were broadly similar to those of Soderberg et al. (2006a), but our observations occurred about 5.5 yr later than theirs, and thus set upper limits on a much later part of the light curve.

3 SN 2003GK

3.1 Additional VLA observations and radio light curve of SN 2003gk

SN 2003gk was the only supernova detected in our radio survey. It was discovered by the Katzmann Automatic Imaging Telescope (KAIT) on 2003 July 1.5 (UT) with an unfiltered magnitude of 17 (Graham & Li 2003a,b). Nothing was seen at its location on a KAIT image from 2002 Dec. 3.2 to magnitude ~ 19 , and an optical spectrum by Matheson et al. (2003) showed it to be probably of Type Ib, resembling SN 1984L several weeks after maximum light, suggesting an explosion date around 2003 June 01 (MJD = 527 92), which date we adopt here. Sollerman et al. (2003), deduced a relatively low expansion velocity of ~ 8300 km s^{-1} from the minimum of the He I 587.6 nm absorption trough. The SN occurred in the Sc galaxy NGC 7460, which is at a distance of 45 Mpc (HyperLeda, Patrel et al. 2003).¹ In order to confirm our radio detection and to determine a light curve and a measure the radio spectral index, we obtained two additional short VLA observations. The first followup observation was on 2010 May 5 (observing code AB1351), where we observed at 8.46 and 22.5 GHz with a total bandwidth of 512 MHz, and the array in the D configuration. The second was on 2012 May 30,

¹ The distance is derived from the measured radial velocities, corrected for the local cluster’s infall velocity to Virgo; obtained from the HyperLeda data base at <http://leda.univ-lyon1.fr>

Table 1. Observed supernovae.

Supernova	Galaxy	Type ^a	D^b (Mpc)	Age ^c (yr)	8.5 GHz flux density ^d (μ Jy)
SN 2001ej	UGC 3829	Ib	57	7.7	<145
SN 2001is	NGC 1961	Ib	56	7.4	<161
SN 2002J	NGC 3464	Ic	56	7.4	<246 (87 \pm 53)
SN 2002bl	UGC 5499	Ic/BL	71	7.3	<357
SN 2002cp	NGC 3074	Ibc	76	7.2	<263
SN 2002hf	MCG-05-3-20	Ic	76	6.6	<241
SN 2002hn	NGC 2532	Ic	75	6.6	< 93
SN 2002ho	NGC 4210	Ic	43	6.7	<266
SN 2002hy	NGC 3464	Ib pec	56	6.6	<247
SN 2002hz	UGC 12044	Ic	76	6.7	<195
SN 2002ji	NGC 3655	Ib/c	28	6.5	<272
SN 2002jj	IC 340	Ic	55	6.5	<208
SN 2002jp	NGC 3313	Ic	55	6.6	<227
SN 2003H	NGC 2207	Ib pec	38	6.4	<188
SN 2003dr	NGC 5714	Ib/c pec	38	6.2	<177
SN 2003gf	MCG-04-52-26	Ic	37	6.1	<213
SN 2003gk	NGC 7460	Ib	44	6.0	2260 \pm 130
SN 2003hp	UGC 10942	Ic/BL	93	5.9	<201
SN 2003id	NGC 895	Ic pec	30	5.7	<278
SN 2003ig	UGC 2971	Ic	79	5.8	<244 (106 \pm 46)
SN 2003ih	UGC 2836	Ib/c	68	5.7	<120
SN 2003jd	NGC 132	Ic/BL	77	5.7	<172
SN 2003jg	NGC 2997	Ib/c	13	5.7	<330
SN 2004ao	UGC 10862	Ib	30	5.4	<256
SN 2004aw	NGC 3997	Ic/BL	73	5.1	<211
SN 2004bm	NGC 3437	Ic	24	5.0	<314
SN 2004bf	UGC 8739	Ic	77	5.3	<460 (154 \pm 102)
SN 2004bs	NGC 3323	Ib	77	5.2	<246
SN 2004bu	UGC 10089	Ic/BL	84	5.0	<244
SN 2004dn	UGC 2069	Ic	51	4.9	<196
SN 2004fe	NGC 132	Ic	72	4.6	<278
SN 2004ge	UGC 3555	Ic	67	4.6	<180
SN 2004gt	NGC 4038	Ic	23	4.5	<593 ^e
SN 2004gv	NGC 856	Ib	79	4.5	<280 (106 \pm 58)
SN 2005E	NGC 1032	Ib/c	36	4.4	<267
SN 2005N	NGC 5420	Ib/c	76	4.8	<285
SN 2005V	NGC 2146	Ib/c	17	4.4	<750 ^e
SN 2005aj	UGC 2411	Ic	38	4.4	<143
SN 2005ct	NGC 207	Ic	54	4.0	<327
SN 2005da	UGC 11301	Ic/BL	68	3.9	<309
SN 2005dg	ESO 420-3	Ic	56	3.9	<370 (121 \pm 83)
SN 2005ek	UGC 2526	Ic	67	3.7	<171
SN 2005eo	UGC 4132	Ic	74	3.8	<200
SN 2005kz	MCG+08-34-32	Ic/BL	115	3.6	<242
SN 2005lr	ESO 492-02	Ic	36	3.5	<185
SN 2006F	NGC 935	Ib	55	3.5	<268
SN 2006ab	PGC 10652	Ic	68	3.3	<159
SN 2006dg	IC 1508	Ic	58	3.2	<180
SN 2006dj	UGC 12287	Ib	73	3.2	<195
SN 2006eg	CGCG462-023	Ibc	53	2.9	<214
SN 2006ep	NGC 214	Ib	61	2.7	<284
SN 2007D	UGC 2653	Ic/BL	93	2.5	<171
SN 2007Y	NGC 1187	Ib	18	2.3	<177
SN 2007iq	UGC 3416	Ic	57	1.9	<126
SN 2007ke	NGC 1129	Ib	70	1.7	<146
SN 2007ru	UGC 12381	Ic/BL	64	1.5	<232
SN 2007rz	NGC 1590	Ic	52	1.6	<170
SN 2008du	NGC 7422	Ic	66	0.9	<412(136 \pm 92)
SN 2008dv	NGC 1343	Ic	33	1.0	<450

^aThe SN type, taken from Barbon et al. (2010), with ‘BL’ indicating a broadline SN. ^bThe distance to the SN, derived from the NED data base. ^cThe age of the SN, since estimated shock breakout or detection the date of observation, on 2009 May 25. ^dThe observed 8.5 GHz flux density and its uncertainty, or the 3σ upper on it. ^eThe flux density from the SN has been corrected for significant radio emission from the galaxy at the location of the SN.

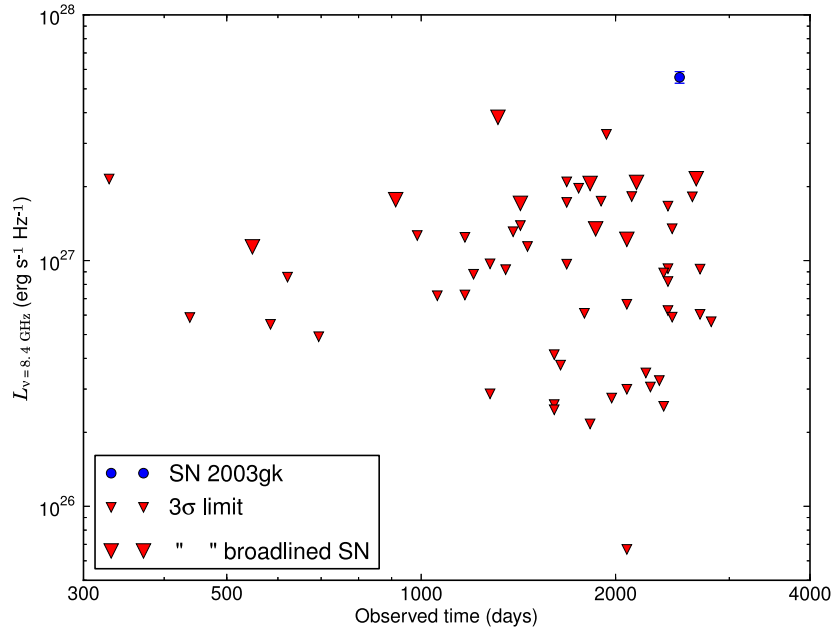


Figure 1. The detection of, and upper limits on the late-time radio emission of Type b/c SNe. We plot the 8.5 GHz spectral luminosity of the sole detection in our sample, SN 2003gk, in blue (note that the error bars are comparable in size to the plotted symbol), and the 3σ upper limits for the remaining 58 SNe as red triangles, plotted against the time of observation relative to the time of the SN explosion. Broadlined SNe are marked with larger triangles.

Table 2. Flux density measurements of SN 2003gk.

Date	MJD	Frequency (GHz)	Flux density ^a (μJy)
2003 07 14	528 34	8.46	$<1980^b$
2009 05 29	549 81	8.46	2280 ± 110
2010 05 02	553 18	8.46	2300 ± 130
2010 05 02	553 18	22.46	1360 ± 90
2012 05 30	560 77	8.46	1450 ± 80
2012 05 30	560 77	21.36	0960 ± 50

^aThe listed uncertainties include an assumed 5 per cent uncertainty in the flux density calibration.

^b 3σ upper limit.

using the VLA wideband system, and we observed at 3, 8, 21 GHz, with a total bandwidth of 2 GHz. In both cases, we used 3C 48 as a flux-density calibrator (using the Perley-Butler 2010 coefficients), and we used J2257+0243 as a phase and delay calibrator, and we used referenced pointing at 18 GHz and higher. The 2010 data set was reduced using Astronomical Image Processing System (AIPS), while the 2012 data set was reduced using CASA (McMullin et al. 2007).

We collect the flux density measurements of SN 2003gk in Table 2 and plot them in Fig. 2. The mean value of the spectral index between 22.5 and 8.5 GHz was -0.5 ± 0.1 .

3.2 VLBI observations

In order to determine the size of the radio emitting region in SN 2003gk, and thus to determine its average expansion speed, we obtained 8.4 GHz VLBI imaging observations of it on 2011 April 21 (observing code BB296), with a total time of 5 h. The mid-point of the observations was at MJD 556 73. We used the High-Sensitivity Array, which consisted of the NRAO VLBA (8×25 m diameter; the Pie Town and North Liberty antennas did not

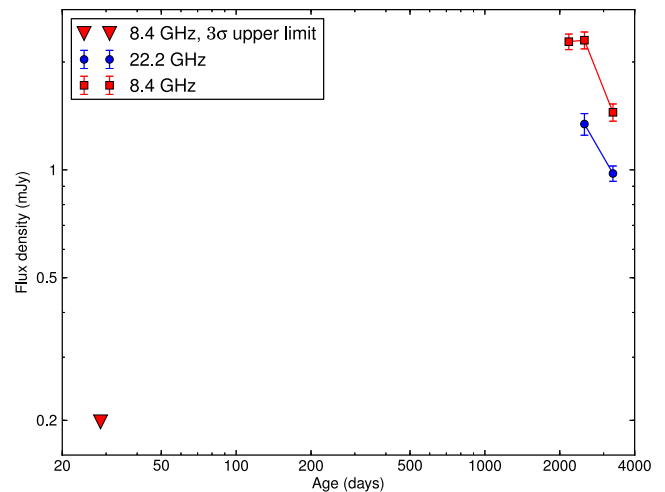


Figure 2. The radio light curves of SN 2003gk at 8.4 and 22 GHz. We plot the measured values with uncertainties as well as the upper limit obtained from the early non-detection in 2003.

take part in this run), the NRAO Robert C. Byrd ~ 105 m telescope at Green Bank, the Effelsberg² (100 m diameter) telescope and the Arecibo³ (305 m diameter) telescopes.

We recorded a bandwidth of 64 MHz in both senses of circular polarization with two-bit sampling, for a total bit rate 512 Mbit s^{-1} . The VLBI data were correlated with NRAO's VLBA processor, and the analysis carried out with NRAO's AIPS. The initial flux

²The telescope at Effelsberg is operated by the Max-Planck-Institut für Radioastronomie in Bonn, Germany.

³The Arecibo Observatory is part of the National Astronomy and Ionosphere Center, which is operated by Cornell University under a cooperative agreement with the National Science Foundation.

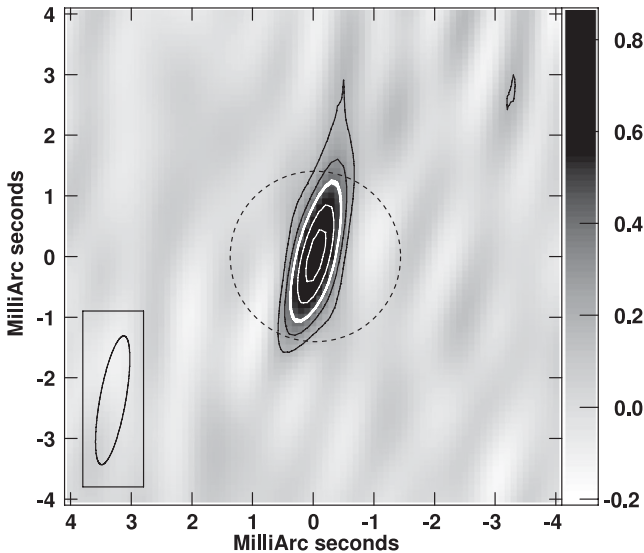


Figure 3. A VLBI image of SN 2003gk taken on 2011 April 21. The contours are drawn at $-20, 20, 30, 50, 70$ and 90 per cent of the peak brightness, which was $86 \mu\text{Jy bm}^{-1}$. The rms background brightness was $51 \mu\text{Jy bm}^{-1}$. The FWHM restoring beam of $2.16 \text{ mas} \times 0.43 \text{ mas}$ is indicated at lower left. North is up and east is to the left, and the coordinate origin is the brightness peak of SN 2003gk, which was at RA = $23^{\text{h}}01^{\text{m}}42^{\text{s}}.98207$, Dec. = $02^{\circ}16'08''.6798$ (J2000). The dashed circle shows a circle of one light-year radius, showing the expected size of a source which has expanded relativistically for one year.

density calibration was done through measurements of the system temperature at each telescope, and then improved through self-calibration of the reference source. A correction was made for the dispersive delay due to the ionosphere using the AIPS task TECOR, although the effect at our frequency is not large.

We phase-referenced our VLBI observations to QSO J2257+0243, which is an ICRF source for which we use the position RA = $22^{\text{h}}57^{\text{m}}17^{\text{s}}.563103$, Dec. = $02^{\circ}43'17''.51172$ (J2000) (Fey et al. 2004). We used a cycle time of ~ 3.9 min, with ~ 2.4 min spent on SN 2003gk. We discarded any SN 2003gk data taken at elevations below 10° . In addition, we also spent two periods of ~ 10 min observing an astrometric check source JVAS J2258+0203, phase-referenced to J2257+0243 in the same manner as SN 2003gk.

We found that on both our check source, JVAS J2258+0203, and for SN 2003gk, the visibility phases for baselines involving Arecibo (AR) showed large residuals, suggesting that phase referencing at AR was not successful, and we therefore did not use the AR data for any astrometric results.

We show the VLBI image of SN 2003gk in Fig. 3. For marginally resolved sources, such as SN 2003gk, the best values for the source size come from fitting models directly to the visibility data, rather than from imaging. We chose as a model the projection of an optically thin spherical shell of uniform volume emissivity, with an outer radius of 1.25 times the inner radius.⁴ Such a model has been found to be appropriate for other radio SNe (see e.g. Bietenholz, Bartel & Rupen 2003; Bartel & Bietenholz 2008). The Fourier transform

⁴ Our results do not depend significantly on the assumed ratio between inner and outer radii, as the effect of reasonable variations in this ratio is considerably less than our stated uncertainties. For a discussion of uncertainties on the shell-size obtained through $u-v$ plane model-fitting compared with those obtained in the image plane for the case of SN 1993J, showing that superior results are obtained using the former, see Bietenholz et al. (2010a).

of this shell model is then fitted to the visibility measurements by least squares.

We obtained a value of 0.37 mas for the outer angular radius of SN 2003gk. We also fitted the same shell model, but added antenna amplitude gains (non-time-dependent scale factors) as free parameters, which changed the fitted outer radius by $+0.06 \text{ mas}$. Since the signal-to-noise ratio is too low to allow reliably fitting antenna gains (a form of amplitude self-calibration), we keep the original value of 0.37 mas as our best-fitting value, but take as a conservative uncertainty the 0.06 mas difference between the value obtained with the antenna gains added as free parameters and the original one. This value is approximately twice as large as the purely statistical uncertainty. We therefore take the final fitted value of the outer angular radius of SN 2003gk as $0.37 \pm 0.06 \text{ mas}$.

For a partially resolved source such as SN 2003gk, the exact model geometry is not critical, and our shell model will give a reasonable estimate of the size of any circularly symmetric source, with a scaling factor of order unity dependent on the exact morphology (see discussion in Bartel et al. 2002). In particular, using a circular Gaussian model instead of the spherical shell model would result in a fitted FWHM size of 0.5 mas , with the same relative uncertainty of 16 per cent. We also attempted a fit of an elliptical Gaussian to model a possibly elongated source. To reduce the number of free parameters, we fixed the axis ratio to 0.2. We obtained an FWHM major axis size of $0.61 \pm 0.10 \text{ mas}$.

Our fitted angular outer radius for SN 2003gk was $0.37 \pm 0.06 \text{ mas}$ (for a spherical shell model). At a distance of 44 Mpc , this corresponds to $(2.4 \pm 0.4) \times 10^{17} \text{ cm}$. The age of the SN at the time of the VLBI observations was 2881 d , so the average expansion velocity was $(1.0 \pm 0.2) \times 10^4 \text{ km s}^{-1}$. The measured radius is not compatible with any relativistic, or near-relativistic expansion: at an apparent speed of c it would have reached our measured size at $t = 96 \text{ d}$, so any reasonable non-relativistic expansion speed in the $\sim 7.5 \text{ yr}$ since then would have increased the size well beyond our measured value. The measured size is, however, entirely compatible with the expansion velocities of ordinary, non-relativistic SNe (e.g. Bietenholz 2005; Bartel 2009). Our VLBI measurements, therefore, exclude any relativistically expanding jet component in SN 2003gk. Unfortunately, with only single epoch of VLBI observations, we cannot constrain the proper motion.

4 CALCULATION OF MODEL LIGHT CURVES

The association of GRBs with massive stars implies that the afterglow shock propagates into the pre-explosion stellar wind, and suggests a stratified external medium with a density profile $\rho_{\text{ext}} = Ar^{-k}$. If the ratio of wind velocity, v_w , to mass-loss rate, \dot{M}_w , remains constant, then $k = 2$ and $A = \dot{M}_w / (4\pi v_w) = 5 \times 10^{11} A_* \text{ g cm}^{-1}$. Since \dot{M}_w / v_w might vary before the SN explosion, and is rather uncertain, other values of k have also been considered both in modelling of GRB afterglows (e.g. Yost et al. 2003; Starling et al. 2008; Leventis et al. 2012, 2013) and recently also in hydrodynamic simulations (De Colle et al. 2012b).

Nonetheless, most afterglow light curves calculated so far, and in particular those from hydrodynamic simulations, have been done for a uniform external medium ($k = 0$). Therefore, we present here results for a wind-like external medium of constant \dot{M}_w / v_w (i.e. $k = 2$), as a representative value for what might more realistically be expected for the wind of a massive star progenitor.

The typical value of the external density normalization parameter, A_* , is usually taken to be 1.0 in modelling, although the values that

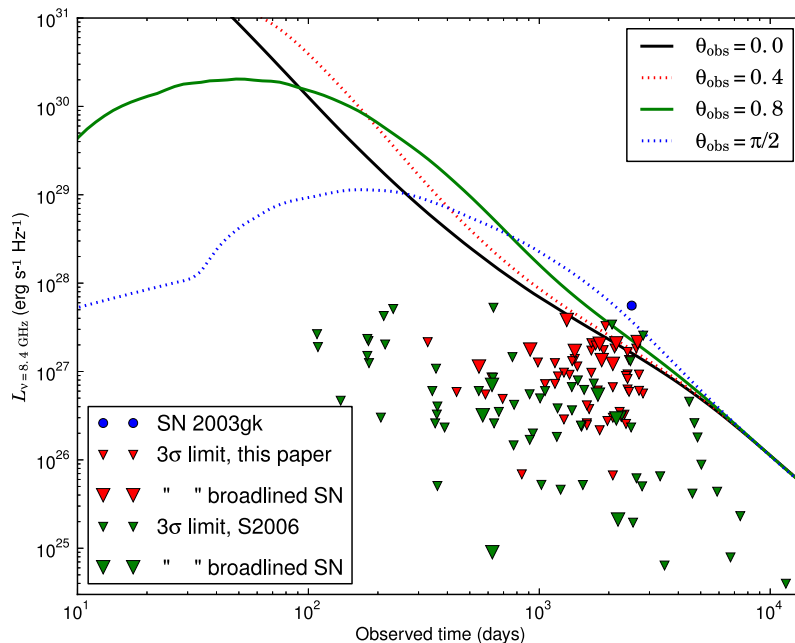


Figure 4. The modelled 8.4 GHz light curves of relativistic jets for angles to the line of sight between 0 and $\pi/2$ rad, as indicated at top right. The light curves were calculated assuming a wind-stratified medium ($k = 2$) with $A_* = 1$ and $\epsilon_B = \epsilon_e = 0.1$ (see the text in Section 4). The red triangles show our upper limits while the blue point is the measured values for SN 2003gk, repeated from Fig. 1 above. We add here the corresponding limits from Soderberg et al. (2006a, marked ‘S2006’) as green triangles. The larger triangles again represent broadlined SNe. Note that for 14 SNe, there are two separate limits, one from our observations and an earlier one from Soderberg et al. (2006a). Although some of our limits (red triangles) are above the modelled light curves, in each such case there is an earlier limit (green triangle) which is well below the modelled curves.

are inferred from afterglow broad-band modelling range from $A_* \simeq 1$ down to less than 0.01. (Kumar & Panaitescu 2003; Chevalier, Li & Fransson 2004; Waxman 2004a,b; Rol et al. 2007; Racusin et al. 2008; Pandey et al. 2009; Cenko et al. 2010, 2011).

The true jet kinetic energy is usually inferred to be $E_{\text{jet}} \sim 10^{50} - 10^{51.5}$ erg, for bright well-monitored afterglows and up to $\sim 10^{52}$ erg for the most energetic afterglows (e.g. Panaitescu & Kumar 2001a,b; Yost et al. 2003; Cenko et al. 2010, 2011). However, low-luminosity GRBs that have a larger rate per unit volume extend this distribution down to $\lesssim 10^{48}$ erg (e.g. Hjorth 2013).

The shock-microphysics processes responsible for field amplification and particle acceleration are typically parametrized by the assumptions that the magnetic field everywhere in the shocked region holds a fraction $\epsilon_B = 0.1$ of the local internal energy density in the flow, and that the non-thermal electrons just behind the shock hold a fraction $\epsilon_e = 0.1$ of the internal energy and have a power-law energy distribution with $N(E) \propto E^{-p}$. When it is possible to infer the values of these microphysics parameters for particular bursts, they are typically in the ranges $10^{-5} \lesssim \epsilon_B \lesssim 10^{-1}$, $10^{-2} \lesssim \epsilon_e \lesssim 10^{-0.5}$ and $2 \lesssim p \lesssim 3$ (e.g. Santana, Barniol Duran & Kumar 2014). We refer to the values $E_{\text{jet}} = 2 \times 10^{51}$ erg, $A_* = 1$, $\epsilon_B = \epsilon_e = 0.1$, which are often used in modelling, as the ‘canonical’ values, although, as just mentioned, they are likely not representative of the majority of bursts.

We use 2D hydrodynamic simulations for $k = 2$ from De Colle et al. (2012b), based on the special relativistic hydrodynamics code MEZCAL, and a complimentary code for calculating the radiation by post-processing the results of the numerical simulations (De Colle et al. 2012a). The GRB was initialized on a conical wedge of half-opening angle $\theta_0 = 0.2$ rad, taken out of the spherical self-similar

Blandford & McKee (1976) solution. The simulation starts when the Lorentz factor of the material just behind the shock was $\Gamma = 20$. The calculation of the synchrotron radiation is supplemented by adding the contribution from a Blandford & McKee (1976) conical wedge at earlier times, corresponding to $20 \leq \Gamma \leq 500$ (which causes an artificially sharp transition in the light curve between the two at a rather early time). Our value of $\theta_0 = 0.2$ corresponds to a beaming factor of $f_b = 1 - \cos \theta_0 \approx 0.02$. The simulation was for $E_{k,\text{iso}} = 10^{53}$ erg, corresponding to $E_{\text{jet}} = f_b E_{k,\text{iso}} \approx 2 \times 10^{51}$ erg, and for $A_* = 1.65$, but was scaled to arbitrary values of E_{jet} and A_* using appropriate scaling relations from Granot (2012). We have fixed the power-law index of the accelerated electrons to $p = 2.5$ as a representative value.

Fig. 4 shows light curves for different viewing angles ($\theta_{\text{obs}} = 0, 0.4, 0.8, \pi/2$) for our optimistic model using the canonical parameters which produce relatively bright radio afterglow emission: $\epsilon_B = \epsilon_e = 0.1$, $E_{k,\text{iso}} = 10^{53}$ erg and $A_* = 1$. In Fig. 5, we fix $\epsilon_B = \epsilon_e = 0.1$ (as well as $\theta_{\text{obs}} = \pi/2$) and show the effect of varying the jet energy ($E_{k,\text{iso}} = 10^{51}, 10^{53}$ erg) and the external density normalization ($A_* = 0.01, 0.1, 1$), to cover a range that might be considered more typical for GRB jets. Hydrodynamic features, such as the observed non-relativistic transition time (which typically corresponds to the peak of the light curve for large off-axis viewing angles) scale as $(E_{k,\text{iso}}/A_*)^{1/(3-k)}$, and therefore they vary much more strongly for the wind-like external medium (as $E_{k,\text{iso}}/A_*$ for $k = 2$) than for a uniform medium where they vary only as $(E_{k,\text{iso}}/n_{\text{external}})^{1/3}$. Not only the peak time varies substantially, but also the peak flux, which depends very strongly on A_* . Fig. 6 fixes $E_{k,\text{iso}} = 10^{52}$ erg and $A_* = 0.1$ (as well as $\theta_{\text{obs}} = \pi/2$), and shows the dependence of the light curves on ϵ_B and ϵ_e when varying the

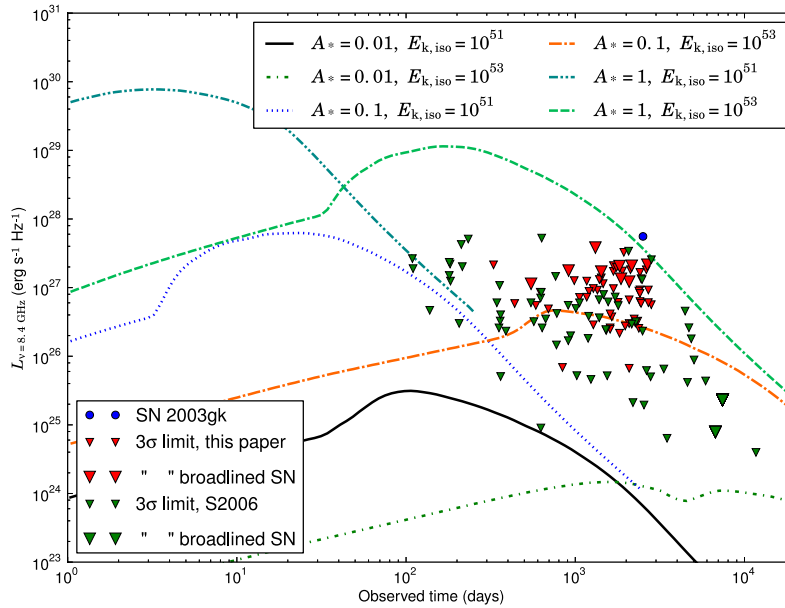


Figure 5. The modelled light curves for various possible explosion energies and circumstellar densities, all for an angle to the line of sight $\theta_{\text{obs}} = \pi/2$. The curves are for the indicated values of $E_{k, \text{iso}}$, the isotropic explosion energy in erg and for a circumstellar density parameter A_* . For comparison, we again plot the observed value for SN 2003gk and limits for the other SNe from our sample (see Fig. 4).

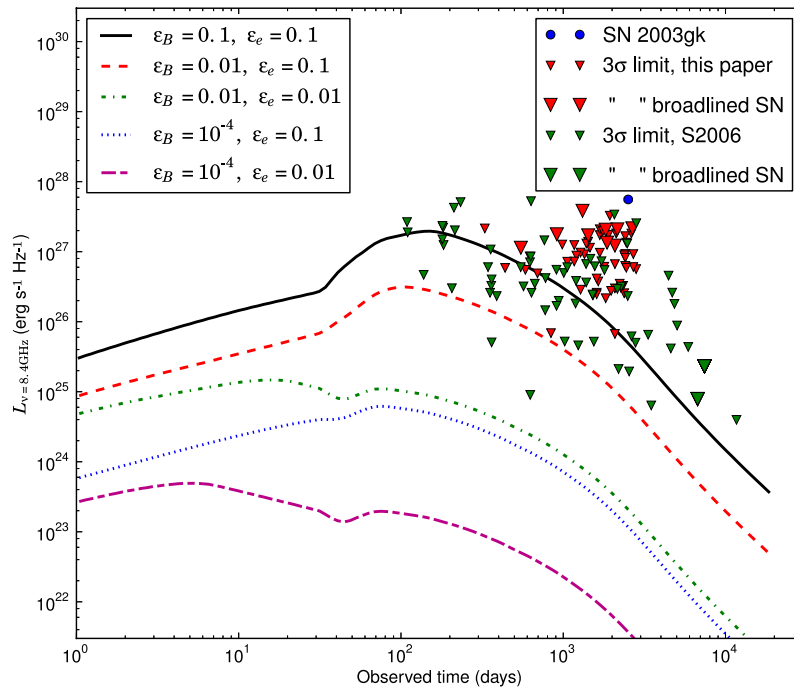


Figure 6. The modelled light curves for various possible efficiencies of magnetic field generation (ϵ_B) and particle acceleration (ϵ_e) at the shock front. All the light curves are for a wind-stratified medium ($k = 2$), $A_* = 0.1$, $E_{k, \text{iso}} = 10^{52}$ erg and for $\theta_{\text{obs}} = \pi/2$. The light curves are shown for the indicated values of (ϵ_B and ϵ_e). For comparison, we again plot the observed value for SN 2003gk and limits for the other SNe from our sample (see Fig. 4).

latter two well within the typical range inferred from GRB afterglow observations ($10^{-4} \leq \epsilon_B \leq 0.1$ and $10^{-2} \leq \epsilon_e \leq 0.1$). This variation also has a large effect on the peak luminosity.

The peak time of the modelled light curves depends on ($E_{k, \text{iso}}/A_*$) and with larger values of this ratio producing later peaks. The light curve with the canonical values of $E_{k, \text{iso}} = 10^{53}$ erg and $A_* = 1$ peaks at $t = 109$ d with 8.4 GHz spectral luminosity, $L_{8.4 \text{ GHz}} =$

1.1×10^{29} erg $\text{s}^{-1} \text{ Hz}^{-1}$, while the faintest of the light curves, also with $E_{k, \text{iso}} = 10^{53}$ erg $\text{s}^{-1} \text{ Hz}^{-1}$ but with $A_* = 0.01$ peaks at $t = 1466$ d and $L_{8.4 \text{ GHz}} = 1.5 \times 10^{24}$ erg $\text{s}^{-1} \text{ Hz}^{-1}$. The light curve with $E_{k, \text{iso}} = 10^{51}$ erg and $A_* = 1$ peaks as early as 3 d with $L_{8.4 \text{ GHz}} = 8 \times 10^{29}$ erg $\text{s}^{-1} \text{ Hz}^{-1}$. In addition, if either ϵ_B or ϵ_e are below the nominal values of 0.1, a fainter light curve results, and the delayed peak, which is characteristic of jets at large angles

to the line of sight, becomes less prominent. This occurs since the peak frequency, $\nu_m \propto \epsilon_B^{1/2} \epsilon_e^2$, and therefore is lower and passes the frequency of observation earlier, before the time when the beaming cone of the jet's radiation reaches our line of sight.

5 COMPARISON OF OBSERVED LIMITS TO MODEL LIGHT CURVES

We now compare the model light curves for relativistic jets at various angles to the line of sight to the measurements of the late time radio emission of Type I b/c SNe. We combine our own sample (Section 2.2 above) with that of Soderberg et al. (2006a). Our combined sample consists of 126 upper limits on 112 different SNe (14 SNe have limits obtained at two different times). We exclude SN 2003gk from this discussion, because as we have shown, its radio emission is not due to a relativistic jet.

The model light curves are strongly dependent on the explosion energy, $E_{k, \text{iso}}$ and the circumstellar density normalization, A_* . We first adopt 'canonical', or optimistic, values of $E_{k, \text{iso}} = 10^{53}$ erg and $A_* = 1$, and show the resulting light curves, along with the observed upper limits, in Fig. 4. If we assume that the jets are randomly oriented, and that the statistics are Gaussian, we can calculate the probability (P) that any such jet would fall below the limits we measured for our sample of SNe. The SN most compatible with the canonical light curves by this criterion is the non-broadlined SN 1996D, with $P \simeq 0.014$, while for broadlined ones it is SN 2003hp with $P \simeq 10^{-4}$. We can therefore conclude that the probability of any of 112 our SNe being as bright as our canonical light curves is < 2 per cent, and that probability that any of the 13 broadlined SNe being as bright is $< 10^{-3}$. Note that a few of the limits from this paper are above the model light curves, but only for SNe for which an earlier limit for the same SN from Soderberg et al. (2006a) was well below the model light curves (as noted, we exclude SN 2003gk here, which is well above the predicted light curves, but as we showed above does not have any relativistic jet).

The brightness of the modelled light curves, however, depends strongly on the explosion energy ($E_{k, \text{iso}}$) and the density of the circumstellar medium (A_*). The canonical values above were adopted for observed GRB afterglows, and almost certainly represent present particularly bright GRB jets rather than the typical ones. In Fig. 5, we therefore show the model light curves for a variety of plausible values for $E_{k, \text{iso}}$ and A_* .

As can be seen, regardless of the value of A_* , all the light curves with $E_{k, \text{iso}} = 10^{51}$ erg are compatible with most of our observed limits, and even the light curves with the canonical value of $E_{k, \text{iso}} = 10^{53}$ erg are compatible with most of our limits provided that the CSM density is characterized by $A_* \lesssim 0.1$. Even for the canonical values of $E_{k, \text{iso}} = 10^{53}$ erg and $A_* = 1$, the predicted light curves fall below many of our measured limits if either ϵ_B or ϵ_e is below the canonical value of 0.1, but still within the range inferred to actually occur in GRBs.

6 DISCUSSION

6.1 SN 2003gk

SN 2003gk was not detected in the radio early on, with an upper limit to the 8.4 GHz spectral luminosity of $L_{8.4 \text{ GHz}} = 4 \times 10^{25}$ erg $\text{s}^{-1} \text{ Hz}^{-1}$ at $t = 29$ d. By $t = 2881$ d, the radio luminosity had risen to $\sim 4 \times 10^{26}$ erg $\text{s}^{-1} \text{ Hz}^{-1}$, and appeared to be decaying rapidly, with $L_{8.4 \text{ GHz}} \propto t^{1.7 \pm 0.3}$ between $t = 2510$ and 3270 d. The spectral index between 8.4 and 22 GHz was -0.6 ± 0.2 .

Our VLBI measurements (Section 3.2) showed that SN 2003gk was expanding non-relativistically, with an average speed of $(1.0 \pm 0.2) \times 10^4$ km s^{-1} . If we assume a power-law expansion, with radius $\propto t^m$ and take a typical value of 0.8 (see, e.g. Weiler et al. 2002) for the deceleration parameter, m , then we can calculate that the initial speed ($t = 30$ d) was 20 000 km s^{-1} , which is within the range usually seen for core collapse SNe in general. Type I b/c SNe tend to have somewhat higher speeds than other SNe, with e.g. Chevalier & Fransson (2006) listing a median speed of $\sim 42 000$ km s^{-1} . If we take the expansion speed of SN 2003gk to have been 42 000 km s^{-1} at $t = 30$ d, we can calculate that SN 2003gk must have been fairly strongly decelerated, with $m \simeq 0.6$.

We mentioned SN 2001em earlier, which showed a similar evolution in flux density, but for which the VLBI observations also implied only non-relativistic expansion. We propose for SN 2003gk an explanation similar to that proposed for SN 2001em (see Chugai & Chevalier 2006; Chevalier 2007), namely that the radio emission is produced by the interaction of a normal Type I b/c ejecta with a massive and dense circumstellar shell at some distance from the progenitor. The shell was the result of episodic mass-loss from the progenitor, perhaps from a luminous blue variable like eruptive event. A possible further diagnostic would be if SN 2003gk were to show strong H α emission, with a relatively narrow linewidth, which would be expected to accompany the strong circumstellar interaction.

6.2 What fraction of Type I b/c SNe host a GRB?

We carried out a survey for late-onset radio emission in Type I b/c SNe that might be indicative of an off-axis relativistic jet. Only one of our 59 SNe, SN 2003gk, showed any such radio emission, but our VLBI observations of it rule out relativistic expansion. It is clear therefore, that regardless of orientation, only a small fraction of Type I b/c have a relativistic jet producing bright late-time radio emission, or in other words host a GRB event. This conclusion was already reached earlier, in particular by Soderberg et al. (2004, 2006a). We have combined our present sample with that of Soderberg et al. (2006a), for a combined set of 112 Type I b/c SNe which have been examined for radio emission such as might arise from an off-axis relativistic jet.

We compared limits on radio emission obtained for this combined sample to model light curves for relativistic jets at various angles to the line of sight (Section 5), using numerically modelled light curves based on hydrodynamic simulations, rather than the semi-analytic ones of Soderberg et al. (2006a).

On the basis of our results, the hypothesis that all Type I b/c SNe have radio light curves as bright as the canonical models with $E_{k, \text{iso}} = 10^{53}$ erg, $A_* = 1$ and $\epsilon_B = \epsilon_e = 0.1$ can be rejected with a high level of confidence. Our sample included 13 broadlined Type I b/c SNe, and we can also reject the hypothesis that all broadlined SNe have such bright radio light curves. We performed Monte Carlo simulations with 10 000 trials, a randomly chosen fraction f_{bright} of our sample of 112 SNe having light curves as bright as our canonical models for each trial, with the remainder being unobservably faint. We then compared the simulated brightness values to our observed values or limits, and calculated the probability of that particular trial given the observed values and the uncertainties (assuming a Gaussian distribution for the measurement errors with the values of σ given or implied by the listed 3σ limit in Table 1). We performed such simulations for various values of f_{bright} , with the result that we can say (at the 99 per cent confidence level) that fewer than 5 per cent (i.e. $f_{\text{bright}} < 0.05$) of all Type I b/c SNe, and fewer than

33 per cent of broadlined SNe have radio light curves as bright as those produced by our canonical models. Our conclusions are consistent with those of Soderberg et al. (2006a), who concluded that at most 10 per cent of all Type I b/c SNe are associated with ‘typical’ GRB jets regardless of orientation, where their ‘typical’ GRB jets have radio luminosities similar to those of the canonical models. Soderberg et al. (2006a) further concluded that even of the broadlined SNe, at most a fraction can be associated with a GRB jet.

Our results are also in agreement with the conclusions of Ghirlanda et al. (2013) who compared a simulated population of GRBs⁵ to samples of observed GRBs from *Swift*, *Fermi* GBM and *CGRO* BATSE (1177 GRBs in total). They found that to match the observed rates of bright GRB detections, the rate of GRB events (at any orientation) was ~ 0.3 per cent the rate of local Type I b/c SNe, and ~ 4.3 per cent that of local BL SNe. Although their constraint on the fraction of Type I b/c SNe accompanied by a bright GRB are tighter than ours, the two estimates are complimentary, since the two estimates have differing model dependences. In particular, the radio observations are sensitive to jets with wide range of Γ , whereas the observational constraints used by Ghirlanda et al. were restricted to highly relativistic jets with $\Gamma \gtrsim 100$.

However, the conclusion that the absence of late-time radio emission rules out off-axis GRB bursts in most Type I b/c SNe are based on the assumption of a fairly bright jet, comparable to the *detected* GRB afterglows. Many of the fainter GRB events will go undetected (Wanderman & Piran 2010; Shahmoradi 2013), and radio afterglows are seen only in a fraction of the detected GRBs. In particular, that conclusion was based on the assumption of a relatively energetic burst with $E_{k,iso} = 10^{53}$ erg, with a relatively dense CSM, characterized by $A_* = 1$, and with a shock that efficiently generates magnetic field and relativistic particles. These assumptions apply to the bright end of the detected radio afterglows, and almost certainly overestimate the radio emission produced by the average burst. To estimate the frequency of relativistic jets in Type I b/c SNe, we want to use values representative of the population rather than of the bright detected bursts.

Our model calculations (Section 4) in fact used a wide range of values for the jet characteristics, and should be more representative of the full range of radio brightnesses that might be expected from relativistic jets. They show that, for jets with lower explosion energies, less dense CSM, or lower values of ϵ_B or ϵ_e , than the canonical values, the predicted radio light curves can be several orders of magnitude lower in flux density. We find that the peak 8.4 GHz spectral luminosity, $L_{8.4\text{GHz}}$, of the off-axis relativistic jet can range between 8×10^{29} erg s⁻¹ Hz⁻¹ (for the canonical values of $E_{k,iso}$ and A_*) and 1.4×10^{24} erg s⁻¹ Hz⁻¹ (for $E_{k,iso} = 10^{51}$ erg and $A_* = 0.01$), corresponding respectively to 260 mJy bm⁻¹ to 0.5 μ Jy bm⁻¹ at a distance of 50 Mpc. Note that even for energetic bursts with $E_{k,iso} = 10^{51}$ erg, the radio brightness can be several orders of magnitude lower than the canonical one.

Although analytical studies and simulations for a constant-density CSM predicted that radio emission from a jet in the plane of the sky would peak at $t \simeq 500$ d (Granot & Loeb 2003; van Eerten et al. 2010; van Eerten & MacFadyen 2012), we find that for a wind-like CSM, with $\rho_{ext} \propto r^{-2}$, the peak time depends strongly on the burst energy and CSM density, with the dependence being as

$E_{k,iso}/A_*$, compared to $(E_{k,iso}/\rho_{ext})^{1/3}$ for a uniform density CSM. For our range of values, the 8.5 GHz peak time could be as short as 3 d (for $E_{k,iso} = 10^{53}$ erg and $A_* = 1$, or as long as ~ 4 yr (for $E_{k,iso} = 10^{53}$ erg and $A_* = 0.01$) for $\theta_{obs} = \pi/2$ (for other viewing angles this time changes, as can be seen in Fig. 4). Thus, the model light curves for off-axis relativistic jets overlap with those seen for normal SNe without any relativistic ejecta, which have peak values of $L_{8.4\text{GHz}}$ up to 10^{28} erg s⁻¹ Hz⁻¹ and times to peak as long as 100 d (e.g. Soderberg et al. 2005, 2006b). We note, however, that the radio emission from non-relativistic SNe shows a marked change of spectral index near the peak time as the SN transitions from the optically thick to optically thin regimes, while emission from an off-axis relativistic jet often shows no such change. A peak in the radio flux density not marked by a change in the spectral index from an optically thick value of ($S_\nu \propto \nu^{5/2}$ or ν^2) before the break, to an optically thin value after, may therefore be diagnostic of off-axis jet emission.

We can conclude therefore that at present, late-time radio observations of Type I b/c SNe, even the ones with broad lines such as have been associated with GRBs, place only weak constraints on the presence of any possible off-axis relativistic (GRB-like) jets associated with these objects. In particular, burst energies lower than $E_{k,iso} = 10^{53}$ erg, low-density CSM and lower efficiency of field amplification or particle acceleration at the shock would all produce jets that have only faint radio emission below the present observational limits.

7 CONCLUSIONS

Here is a summary of our main conclusions.

(1) Late-time radio emission was detected from SN 2003gk, with an 8.4 GHz flux density of 2.30 ± 0.13 mJy at age ~ 8 yr. No radio emission was present at the age of ~ 1 month. The late-time radio emission is decaying with time, and has a spectral index of 0.5 ± 0.1 .

(2) VLBI observations of SN 2003gk showed that its average expansion speed at age ~ 8 yr was $10\,000 \pm 2000$ km s⁻¹, which is incompatible with relativistic expansion over more than $t \simeq 100$ d. The speed is, however, comparable to what is seen in normal, non-relativistic SNe. The radio emission is likely due to the SN shock impacting upon a dense shell in the CSM of the progenitor. A diagnostic would be if SN 2003gk were to show strong H α emission with a relatively narrow linewidth.

(3) We surveyed 58 other Type I b/c SNe for late-time radio emission, such as might be produced by an off-axis GRB jet. We combined our results with those of similar, earlier survey by Soderberg et al. (2006a), for a total sample of 112 Type I b/c SNe. None of the 112 Type I b/c SNe surveyed, including 13 broadlined SNe, showed any radio emission attributable to an off-axis GRB jet.

(4) We calculated new model light curves for relativistic jets in a wind-stratified (density $\propto r^{-2}$) circumstellar medium for various angles to the line of sight and for various values of the energy of the burst, the circumstellar density, and the efficiency of magnetic-field amplification and particle acceleration at the shock front.

(5) For canonical parameters, such as are typical of detected GRBs, the predicted radio light curves for jets in the plane of the sky are bright, with peak 8.4 GHz spectral luminosities of 8×10^{29} erg s⁻¹ Hz⁻¹. However, varying the four parameters above within reasonable ranges can reduce the brightness by several orders of magnitude.

⁵ Ghirlanda et al. (2013) synthesized a population of GRBs under the assumption that, in the rest frame, all GRBs emit a total gamma-ray energy of 1.5×10^{48} erg have an νF_ν spectrum that peaks at 1.5 keV.

(6) Based on our simulations, the radio light curves of off-axis relativistic jets overlap with those of ordinary, non-relativistic SNe both in peak luminosity and time to reach the maximum, even for jets in the plane of the sky. The present radio observations therefore do not place any strong constraints on the presence of off-axis jets in Type I b/c SNe.

ACKNOWLEDGEMENTS

Research at Hartebeesthoek Radio Astronomy Observatory was partly supported by National Research Foundation (NRF) of South Africa. Research at York University was partly supported by NSERC. FDC acknowledges support from the DGAPA-PAPIIT-UNAM grant IA101413-2. The National Radio Astronomy Observatory (NRAO) is a facility of the National Science Foundation operated under cooperative agreement by Associated Universities, Inc. The Arecibo Observatory is operated by SRI International under a cooperative agreement with the National Science Foundation (AST-1100968), and in alliance with Ana G. Méndez Universidad Metropolitana and the Universities Space Research Association. We have made use of NASA's Astrophysics Data System Bibliographic Services, the HyperLeda data base and the NASA/IPAC Extragalactic Database (NED) which is operated by the Jet Propulsion Laboratory, California Institute of Technology, under contract with the National Aeronautics and Space Administration.

REFERENCES

- Barbon R., Buondi V., Cappellaro E., Turatto M., 2010, *VizieR Online Data Catalog*, 1, 2024
- Bartel N., 2009, in Hagiwara Y., Fomalont E., Tsuboi M., Yasuhiro M., eds, *ASP Conf. Ser. Vol. 402, Approaching Micro-Arcsecond Resolution with VSOP-2: Astrophysics and Technologies*. Astron. Soc. Pac., San Francisco, p. 243
- Bartel N., Bietenholz M. F., 2008, *ApJ*, 682, 1065
- Bartel N. et al., 2002, *ApJ*, 581, 404
- Bietenholz M., 2005, in Romney J., Reid M., eds, *ASP Conf. Ser. Vol. 340, Future Directions in High Resolution Astronomy*. Astron. Soc. Pac., San Francisco, p. 286
- Bietenholz M. F., 2014, *Publ. Astron. Soc. Aust.*, 31, 2
- Bietenholz M. F., Bartel N., 2005, *ApJ*, 625, L99
- Bietenholz M. F., Bartel N., 2007, *ApJ*, 665, L47
- Bietenholz M. F., Bartel N., Rupen M. P., 2002, *ApJ*, 581, 1132
- Bietenholz M. F., Bartel N., Rupen M. P., 2003, *ApJ*, 597, 374
- Bietenholz M. F. et al., 2010a, *Proc. 10th European VLBI Network Symposium and EVN Users Meeting: VLBI and the New Generation of Radio Arrays*. PoS, Trieste, Italy, available at: http://pos.sissa.it/archive/conferences/125/057/10th%20EVN%20Symposium_057.pdf
- Bietenholz M. F. et al., 2010b, *ApJ*, 725, 4
- Bietenholz M. F., Bartel N., Rupen M. P., 2010, *ApJ*, 712, 1057
- Blandford R. D., McKee C. F., 1976, *Phys. Fluids*, 19, 1130
- Cenko S. B. et al., 2010, *ApJ*, 711, 641
- Cenko S. B. et al., 2011, *ApJ*, 732, 29
- Chandra P., Frail D. A., 2012, *ApJ*, 746, 156
- Chevalier R. A., 1982, *ApJ*, 259, 302
- Chevalier R. A., 1998, *ApJ*, 499, 810
- Chevalier R. A., 2007, in García-Segura G., Ramírez-Ruiz E., eds, *Rev. Mex. Astron. Astrofis. Conf. Ser. Vol. 30, Circumstellar Media and Late Stages of Massive Stellar Evolution*. *Rev. Mex. Astron. Astrofis.*, p. 41
- Chevalier R. A., Fransson C., 2006, *ApJ*, 651, 381
- Chevalier R. A., Li Z., Fransson C., 2004, *ApJ*, 606, 369
- Chugai N. N., Chevalier R. A., 2006, *ApJ*, 641, 1051
- Cobb B. E., Bloom J. S., Perley D. A., Morgan A. N., Cenko S. B., Filippenko A. V., 2010, *ApJ*, 718, L150
- Corsi A. et al., 2014, *ApJ*, 782, 42
- De Colle F., Granot J., López-Cámara D., Ramírez-Ruiz E., 2012a, *ApJ*, 746, 122
- De Colle F., Ramírez-Ruiz E., Granot J., Lopez-Camara D., 2012b, *ApJ*, 751, 57
- Fey A. L. et al., 2004, *AJ*, 127, 3587
- Frail D. A. et al., 2001, *ApJ*, 562, L55
- Gal-Yam A. et al., 2006, *ApJ*, 639, 331
- Galama T. J. et al., 1998, *Nature*, 395, 670
- Gehrels N., Ramírez-Ruiz E., Fox D. B., 2009, *ARA&A*, 47, 567
- Ghirlanda G. et al., 2013, *MNRAS*, 428, 1410
- Graham J., Li W., 2003a, *Cent. Bur. Electron. Telegrams*, 25, 1
- Graham J., Li W., 2003b, *IAU Circ.*, 8162, 2
- Granot J., 2007, in Lee W. H., Ramírez-Ruiz E., eds, *Rev. Mex. Astron. Astrofis. Conf. Ser. Vol. 27, Triggering Relativistic Jets*. *Rev. Mex. Astron. Astrofis.*, p. 140
- Granot J., 2012, *MNRAS*, 421, 2610
- Granot J., Loeb A., 2003, *ApJ*, 593, L81
- Granot J., Ramírez-Ruiz E., 2004, *ApJ*, 609, L9
- Granot J., Panaitescu A., Kumar P., Woosley S. E., 2002, *ApJ*, 570, L61
- Hjorth J., 2013, *Phil. Trans. R. Soc. A*, 371, 20275
- Kumar P., Panaitescu A., 2003, *MNRAS*, 346, 905
- Leventis K., van Eerten H. J., Meliani Z., Wijers R. A. M. J., 2012, *MNRAS*, 427, 1329
- Leventis K., van der Horst A. J., van Eerten H. J., Wijers R. A. M. J., 2013, *MNRAS*, 431, 1026
- MacFadyen A. I., Woosley S. E., Heger A., 2001, *ApJ*, 550, 410
- Malesani D. et al., 2004, *ApJ*, 609, L5
- Matheson T., Challis P., Kirshner R., Hicken M., Calkins M., 2003, *IAU Circ.*, 8164, 2
- McMullin J. P., Waters B., Schiebel D., Young W., Golap K., 2007, in Shaw R. A., Hill F., Bell D. J., eds, *ASP Conf. Ser. Vol. 376, Astronomical Data Analysis Software and Systems XVI*. Astron. Soc. Pac., San Francisco, p. 127
- Mészáros P., 2006, *Rep. Prog. Phys.*, 69, 2259
- Meunier C. et al., 2013, *MNRAS*, 431, 2453
- Nakar E., Piran T., Granot J., 2002, *ApJ*, 579, 699
- Paczyński B., 2001, *Acta Astron.*, 51, 1
- Panaitescu A., Kumar P., 2001a, *ApJ*, 554, 667
- Panaitescu A., Kumar P., 2001b, *ApJ*, 560, L49
- Pandey S. B. et al., 2009, *A&A*, 504, 45
- Paragi Z. et al., 2010, *Nature*, 463, 516
- Paturel G., Petit C., Prugniel P., Theureau G., Rousseau J., Brouty M., Dubois P., Cambrésy L., 2003, *A&A*, 412, 45
- Pian E. et al., 2006, *Nature*, 442, 1011
- Piran T., 2004, *Rev. Mod. Phys.*, 76, 1143
- Racusin J. L. et al., 2008, *Nature*, 455, 183
- Rhoads J. E., 1997, *ApJ*, 487, L1
- Rol E. et al., 2007, *ApJ*, 669, 1098
- Salas P., Bauer F. E., Stockdale C., Prieto J. L., 2013, *MNRAS*, 428, 1207
- Santana R., Barniol Duran R., Kumar P., 2014, preprint ([arXiv:1309.3277](https://arxiv.org/abs/1309.3277))
- Schinzl F. K., Taylor G. B., Stockdale C. J., Granot J., Ramírez-Ruiz E., 2009, *ApJ*, 691, 1380
- Shahmoradi A., 2013, *ApJ*, 766, 111
- Soderberg A. M., 2007, in Immler S., Weiler K., McCray R., eds, *AIP Conf. Ser. Vol. 937, Supernova 1987A: 20 Years After: Supernovae and Gamma-Ray Bursters*. Am. Inst. Phys., New York, p. 492
- Soderberg A. M., Frail D. A., Wieringa M. H., 2004, *ApJ*, 607, L13
- Soderberg A. M., Kulkarni S. R., Berger E., Chevalier R. A., Frail D. A., Fox D. B., Walker R. C., 2005, *ApJ*, 621, 908
- Soderberg A. M., Nakar E., Berger E., Kulkarni S. R., 2006a, *ApJ*, 638, 930
- Soderberg A. M., Chevalier R. A., Kulkarni S. R., Frail D. A., 2006b, *ApJ*, 651, 1005
- Soderberg A. M. et al., 2010a, *Nature*, 463, 513
- Soderberg A. M., Brunthaler A., Nakar E., Chevalier R. A., Bietenholz M. F., 2010b, *ApJ*, 725, 922
- Sollerman J., Andersson J., Gustafsson M., Jakobsson P., Oye G., Patat F., 2003, *IAU Circ.*, 8164, 3
- Stanek K. Z. et al., 2003, *ApJ*, 591, L17

Starling R. L. C., van der Horst A. J., Rol E., Wijers R. A. M. J., Kouveliotou C., Wiersema K., Curran P. A., Weltevrede P., 2008, *ApJ*, 672, 433
Starling R. L. C. et al., 2011, *MNRAS*, 411, 2792
van Eerten H. J., MacFadyen A. I., 2012, *ApJ*, 751, 155
van Eerten H., Zhang W., MacFadyen A., 2010, *ApJ*, 722, 235
van Paradijs J., Kouveliotou C., Wijers R. A. M. J., 2000, *ARA&A*, 38, 379
Wanderman D., Piran T., 2010, *MNRAS*, 406, 1944
Waxman E., 2004a, *ApJ*, 602, 886
Waxman E., 2004b, *ApJ*, 605, L97
Weiler K. W., Panagia N., Montes M. J., Sramek R. A., 2002, *ARA&A*, 40, 387

Woosley S. E., 1993, *ApJ*, 405, 273
Woosley S. E., Bloom J. S., 2006, *ARA&A*, 44, 507
Xu D. et al., 2013, *ApJ*, 776, 98
Yost S. A., Harrison F. A., Sari R., Frail D. A., 2003, *ApJ*, 597, 459
Zhang B., 2007, *Adv. Space Res.*, 40, 1186

This paper has been typeset from a \TeX/L\TeX file prepared by the author.